Journal of
Composites Science

MDPI

Article

Calcium Phosphate-Loaded Novel Polypropylene Glycol-Based Dental Resin Composites: Evaluation of In Vitro Bioactivity

Zahra Shafqat [1], Nadia Munir [1,*], Naveed Inayat [2], Muhammad Adnan Khan [3,*], Muhammad Amber Fareed [4] and Muhammad Sohail Zafar [5]

[1] Department of Dental Materials, Avicenna Dental College, Defense Housing Authority Phase 1X, Lahore 54000, Pakistan; zahrashafqat@gmail.com
[2] Department of Prosthodontics, Avicenna Dental College, Defense Housing Authority Phase 1X, Lahore 54000, Pakistan; naveedinayat092@gmail.com
[3] Department of Dental Materials, Institute of Basic Medical Sciences, Khyber Medical University Peshawar, Peshawar 25100, Khyber Pakhtunkhwa, Pakistan
[4] Department of Restorative Dental Sciences, Gulf Medical University College of Dentistry, Al Jerf 1, Ajman 4184, United Arab Emirates; prof.mafareed@gmu.ac.ae
[5] Department of Restorative Dentistry, College of Dentistry, Taibah University, Al Madina Al Munawara 41311, Saudi Arabia; drsohail_78@hotmail.com
* Correspondence: naaadya3@gmail.com (N.M.); adnan.khan.37@hotmail.com (M.A.K.)

Abstract: Objective: This study aimed to assess in vitro bioactivity of novel remineralizing dental composites loaded with calcium phosphate fillers and chlorhexidine in polypropylene glycol (PPG) resin matrix. Methods: The stock monomer was prepared by adding 69.75% urethane dimethacrylate and 23.25% of the polypropylene glycol dimethacrylate with silica fillers, chlorhexidine (5 wt%), and varying levels of calcium phosphate fillers. The study groups were BC (basic composite), commercial control, CHX-CP5, CHX-CP10, and CHX-CP15, respectively. Bioactivity was assessed by placing samples in the simulated body fluid (SBF) for 7, 14, and 28 days and observed under the scanning electron microscope and energy dispersive X-ray spectroscopy. Data were presented in mean and percentage with a 95% confidence interval. Intergroup analysis was performed using one-way ANOVA and the p-value was set ≤ 0.05. Results: The SEM images showed the deposition of calcium phosphate on the surface of CHX-CP10 and CHX-CP15 after 28 days in SBF. Mineral deposits of calcium and phosphate were observed on the surface of the experimental formulation containing higher calcium phosphate fillers (CP10 and CP15) in EDX. Conclusion: The addition of calcium phosphate fillers to the composites resulted in an apatite layer formed and demonstrated enhanced bioactivity in the presence of PPGDMA and CHX.

Keywords: composite; antibacterial; remineralization; chlorhexidine; calcium phosphate

Citation: Shafqat, Z.; Munir, N.; Inayat, N.; Khan, M.A.; Fareed, M.A.; Zafar, M.S. Calcium Phosphate-Loaded Novel Polypropylene Glycol-Based Dental Resin Composites: Evaluation of In Vitro Bioactivity. *J. Compos. Sci.* **2023**, *7*, 140. https://doi.org/10.3390/jcs7040140

Academic Editor: Masao Irie

Received: 30 December 2022
Revised: 24 March 2023
Accepted: 31 March 2023
Published: 4 April 2023

1. Introduction

Resin-based dental composites (RBDCs) are permanent tooth-colored dental restorative materials. RBDCs have traditionally been known for their high strength and excellent aesthetics [1]. From the standpoint of clinicians, RBDCs are the material of choice due to their ease of manipulation, availability in variety of shades and opacities [2], time savings, quick setting, and patient satisfaction. RBDCs, on the other hand, have a number of disadvantages, including polymerization-induced shrinkage stress [3], limited toughness, mismatch of thermal expansion, fracture, low abrasion resistance, micro-leakage, and monomer toxicity [4]. An organic polymer matrix (produced from dimethacrylate monomers such as UDMA, BisGMA, TEGDMA), inorganic fillers (e.g., glass, ceramic), coupling agents, and the initiator–accelerator system are the four major components of dental composites. Much effort has been put into reconfiguring these components in order to mitigate shrinkage and improve mechanical properties. RBDCs have been subjected

to a variety of modifications, including the addition of bioactive fillers to promote remineralization and enhance longevity of the restoration [5] and antibacterial agents such as chitosan [6], fluoride [7], and chlorhexidine [8].

Polypropylene glycol dimethacrylate (PPGDMA, Polyscience-Illionis, Niles, IL, USA) is a polyether that, like triethylene glycol dimethacrylate (TEGDMA), is used as a diluent monomer in RBDCs. It is more flexible and features a lower double bond concentration than TEGDMA [9]. Because of its high molecular mass, high flexibility, low double bond concentration, and low viscosity, PPGDMA has a high monomer conversion and low shrinkage of the composite material [10]. Human teeth and skeletal tissue are composed of calcium and phosphate, which are osteoconductive in nature; this distinguishing feature has drawn the attention of clinicians and researchers [11]. The minerals monocalcium phosphate monohydrate and tricalcium phosphate are biocompatible and osteoconductive. They are phosphoric acid salts and reactive calcium phosphate fillers [12].

Because of its acidic nature and high solubility at nearly all pH values, mono calcium phosphate monohydrate is used in conjunction with basic calcium compounds such as α-TCP and β-TCP (Biotal Plasma, Maharashtra, India) [13]. When monocalcium phosphate monohydrate is combined with tricalcium phosphate, dicalcium phosphate dihydrate (DCPD) is formed, which is a moldable paste that solidifies to form a hard material [14]. DCPD is widely used in biomedical application domains such as toothpaste as an anticarious agent in combination with fluoride and a polishing agent. When added to dental restorative materials, DCPD promotes remineralization [15].

Studies on β-TCP based biomaterials have validated the higher biocompatibility, when used as resorbable bone implants. They are presently the main component of many bioceramics and composites [13]. In oral and maxillofacial bone regeneration, a combination of monocalcium phosphate and TCP has been tested. Di calcium phosphate dihydrate has been explored in the form of granules to heal bone defects such as post-extraction dental alveolar sockets [8]. Due to their chemical similarities to bones and teeth, calcium phosphate materials have attracted a lot of scientific attention due to the superior biocompatibility and the lesser toxicity of their chemical components. The hydroxyapatite and tricalcium phosphate are the two forms of calcium phosphates that are the most frequently utilized. Calcium phosphates are a class of bioactive synthetic materials, because of their osteoconductivity, crystalline structures, and chemical resemblance to bone microstructure as well tooth enamel. Tricalcium phosphate has been classified as resorbable whereas hydroxyapatite has been classified as nonresorbable [16,17]. The crystalline structure and chemical constitution of calcium phosphate compounds, especially the molar ratio of calcium to phosphorus (Ca/P), are used to classify them [18]. There are many different polymorphs of calcium phosphate, including calcium-deficient hydroxyapatite, dicalcium phosphate, and tricalcium phosphate. However, the frequently researched calcium phosphate compounds in dental composites are beta-tricalcium phosphate (β-TCP) and mono calcium phosphate monohydrate (MCPM, Aldrich) [19,20]. The long-term stability of dental restorations can be increased when TCP is added to dental composites because it can encourage osseointegration. Moreover, β-TCP can enhance the strength properties and fracture toughness of dental resin-based composites.

In this study, a novel polypropylene glycol (PPG)-based dental composite was developed by incorporating reactive calcium phosphate fillers (a mixture of TCP and mono calcium phosphate monohydrate) as a remineralizing agent. Furthermore, the current study investigated the effects of reactive calcium phosphate and the in vitro bioactivity of experimental dental composites because PPG has lower toxicity due to its high molecular weight when compared to triethylene glycol dimethacrylate (TEGDMA) [10]. The use of PPG monomer results in less shrinkage in composites. This may contribute to the longevity of the restoration by enhanced bond strength at the tooth–composite interface [9]. The presence of chlorhexidine assists in the initiation of remineralization by reducing microleakage and maintaining the neutral pH of the surroundings. It also improves bond strength. The hydroxyapatite precipitation and nearly neutral pH may reduce tooth restoration failure

due to less shrinkage, aid demineralised dentine repair and prevent subsurface carious disease, respectively [8].

2. Materials and Methods

This experimental study was carried out at the Interdisciplinary Research Centre in Biomaterials (IRCBM) COMSATS University, Lahore campus Pakistan, with the approval of the PGMI, Lahore Pakistan's ethical committee. The materials used in this project were of analytical grade and were primarily obtained from Sigma Aldrich in the United States.

As a control group, a commercial resin composite (Z250FiltekTM Z2503M A2 shade, Lot#NA02858) was used. All experimental composite preparation procedures, including stock monomer preparation, silica salinization, as well as experimental and composite disc preparation, were carried out at room temperature (23 °C ± 3).

2.1. Salinization of Silica (Filler)

In this study, silica particles were salinized before being mixed with monomer, as described by Cheng et al. [21]. To sum up, silica was salinized using a 10% solution of 3-(trimethoxysilyl) propyl methacrylate (MPS) as a silane coupling agent. This MPS solution was made with 10% MPS, 10% deionized water, and 90% ethanol. The pH of the solution was measured and adjusted to 3.5 by adding 3.0 M acetic acid solution [17] (Daejung Chemicals, Busan, Republic of Korea. CAS# 64-19-7, LOT# A0010MF). A mixer was used to stir the mixture for 30 min (SKU: HTMST100V2 eisco scientific mixer). This solution was then treated with silica powder after 30 min. For 24 h, the solution was stirred with a magnetic stirrer. After that, the solution was filtered and washed with absolute ethanol [22]. Prior to mixing with the monomer, silica was heated at 110 °C to eliminate any remaining moisture.

2.2. Preparation of Experimental Dental Composites Groups

In an amber glass bottle, monomers, initiators, and activators were weighted to a total of approximately 10 gm (10 mL). All of the experimental formulations' liquid phases contained 69.75 wt% urethane dimethacrylate (UDMA, Aldrich), 23.25 wt% polypropylene glycol dimethacrylate (PPGDMA), 5 wt% 3-hydroxyethyl methacrylate (HEMA, Aldrich), 1 wt% dimethyl-p-toluidin, and 1 wt% camphorquinone. From the highest to the lowest fraction, the different constituents were measured in weight percent.

Four experimental groups were created, each with varying levels of calcium phosphate fillers and an equal weight percentage of stock monomer (Table 1). Filtek™ Z250 (UDMA (urethane dimethacrylate)) and Bis-EMA (Bisphenol A polyethylene glycol diether dimethacrylate based composite) were used as commercial controls; stock monomer and fillers were added to 10 mL of 99.5% ethanol in a glass beaker to obtain homogeneous mixture and oven dried silica was added to ethanol and mixed for 10 min for homogeneous mixing, followed by the addition of MCPM and β-TCP and mixed for 10 min. When the mixture was homogenised, chlorhexidine (CHX, Aldrich) was added towards the end. To prevent light activation, aluminium foil was wrapped around the glass beaker. Small holes were drilled in the aluminium covering to allow the ethanol in the mixture to evaporate. The mixture was mixed for 24 h on a hot plate at 450 rpm.

The disc-shaped specimens were formed using Teflon moulds (8 mm × 2 mm). Disc specimens for testing were positioned in tubes with 10 mL simulated body fluid (SBF) and stored at 37 °C.

Table 1. Experimental groups based on the varying levels of calcium phosphate and chlorhexidine.

Abbreviation Formulations	Composition of the Composite	Fillers (wt%)			
		CHX	Silica	CaP	
				MCPM	β-TCP
BC	Basic composite without any reactive fillers (BC)	0	40%	0	0
CHX-CP5	BC + 5% (MCPM) 5% (β-TCP) + 5% Chlorhexidine	5%	40%	5%	5%
CHX-CP10	BC + 10% MCPM, 10% β-TCP + 5% Chlorhexidine	5%	40%	10%	10%
CHX-CP15	BC + 15% MCPM, 15% β-TCP + 5% Chlorhexidine	5%	40%	15%	15%

Abbreviation CP: Calcium phosphate fillers, CHX-chlorhexidine, BC: basic composite without any reactive filler. Monomers in all experimental formulations consist of UDMA, PPGDMA, and HEMA.

2.3. Preparation of Simulated Body Fluid

The SBF was freshly synthesized using the protocol as described by Kokubo and Takadama [23]. Due to its identical ion concentration as human blood plasma, the SBF was used to test the in vitro bioactivity of the experimental RBDCs [24]. At 36.5 °C, buffering agents were 50 Mm TRIS (trishydroxymethyl amino methane) and 45 Mm HCL (buffered at a pH of 7.40). The beaker was placed in a water bath and heated to 36.5 ± 1.5 °C. Once the temperature was reached, the following ingredients were added in the same order: NaCl (8.035 g), $NaHCO_3$ (0.355 g), KCL (0.225 g), K_2HPO_4 (0.176 g), $MgCl{\cdot}6H_2O$ (0.311 g), 1 M HCl (39 mL), $CaCl_2$ (0.292 g), and Na_2SO_4 (0.072 g). The solution was then transferred to a 1000 mL volumetric glass flask and cooled to up to 20 degrees celsius. By adding ion exchange and distilled water, the total volume of the solution was raised to 1000 mL. Finally, the solution was transferred to a polyethylene bottle and refrigerated at 4 °C for a month [23].

2.4. In Vitro Bioactivity Test

The disc's bioactivity was assessed using the ISO 23317:2007 standard to determine apatite formation ability and bioactivity (ISO 23317:2007). For 7, 14, and 28 days, the samples were immersed in SBF to assess the deposition of calcium phosphate filled composite. Composite disc samples were prepared in vials using a Teflon mould with dimensions of 8 mm in width and 2 mm in height. A total of 10 mL of SBF solution was measured and added to each vial with discs immersed before being placed in the incubator at 37 °C. After a specific time of immersion, the samples were removed from the incubator, gently rinsed for 1 min with deionized water, and then dried at 100 °C for 2 h [25]. After dehydration, the surface morphology of the specimen was assessed using a scanning electron microscope (Tescan Vega-3, Tescan, Brno, Czech Republic, LMU, CR) and the sample was gold coated in a gold sputter coater (Quorum, Lewes, UK). SEM scans were performed at a magnification of 1500× (20 m) and an accelerated voltage of 5 KV. The same specimens were assessed for elemental analysis using an energy dispersive X-ray (EDX) at 20 kV.

2.5. Statistical Analysis

Data were presented in mean and percentage with a 95% confidence interval. Intergroup analysis was performed using a one-way ANOVA to compare the means of study groups in order to determine the statistical evidence that the means are significantly different. The p-value was set ≤ 0.05 to determine that the results were statistically significant. All

values were presented in the form of tables and charts. Three samples per group, including control and experimental groups each, for SEM and EDX were assessed [8].

3. Results

3.1. SEM and EDAX Analysis for In Vitro Bioactivity

After 7, 14, and 28 days of storage in SBF, the in vitro bioactivity of all groups was analysed and compared using SEM and EDAX. Figure 1 shows SEM images after 7 days of immersion in SBF. At day 7, all sample groups had minor roughness with no apatite layer formation on the disc's surface. The disc surfaces of groups Filtek Z250 and BC were smooth, but the surfaces of groups CHX-CP5, CHX-CP10, and CHX-CP15 have porosities. This could be due to the formation of air bubbles during mixing or, the substantial porosity structure of MCPM particles.

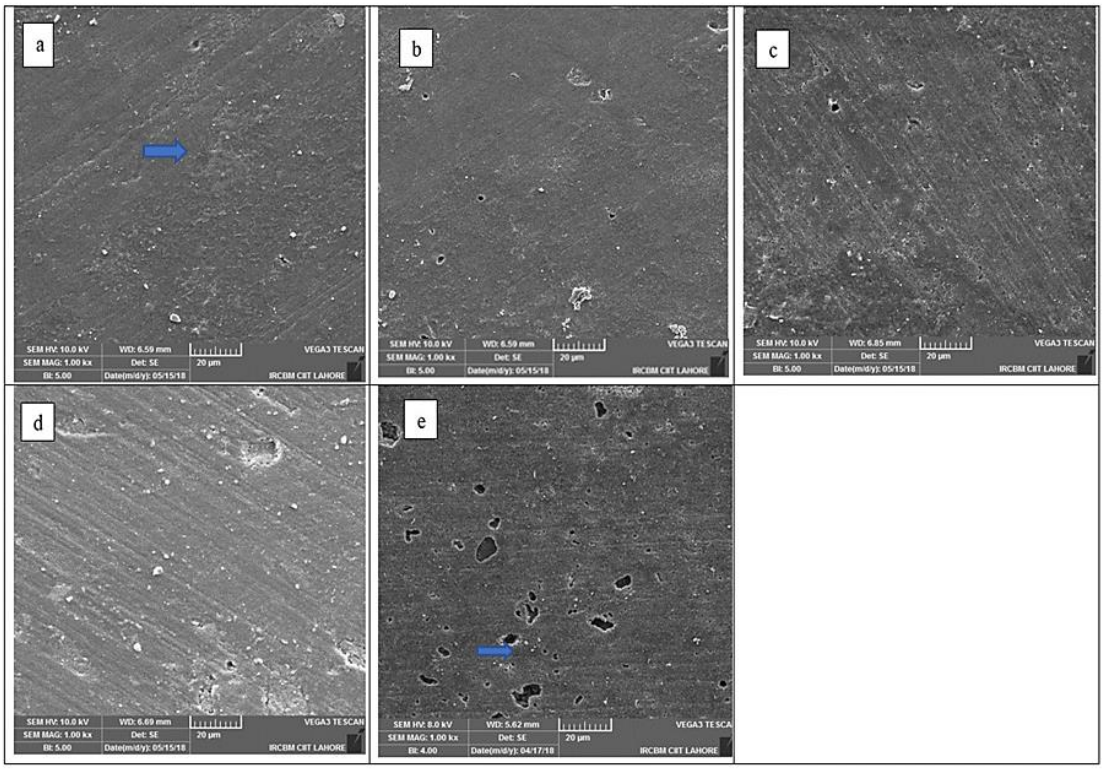

Figure 1. Shows the SEM surface analysis of (**a**) Z250, (**b**) BC, (**c**) CHX-CP5, (**d**) CHX-CP10 and (**e**) CHX-CP15 at day 7. There was no apatite layer formation on the surface of all the groups. The arrows indicate slight roughness and porosities. Images are taken at 1000× magnification.

Figure 2 depicts SEM images of the commercial and experimental formulations after 14 days in SBF immersion. Small surface deposits on the surface of Z250 and group BC on day 14. As the calcium phosphate filler level increased, so did the deposit of smaller particles on the surface. Furthermore, higher calcium phosphate filler levels increased surface porosities as shown by the arrow in CHX-CP15.

Figure 3 shows SEM images of commercial and experimental formulation surfaces after 28 days in SBF. Surface SEM images from groups Z250, BC, and CHX-CP5 revealed a few deposits of a smaller particle-shaped structure. However, as the calcium phosphate level increased, the size of the surface irregularities increased, noticeably in the CHX-CP10 and CHX-CP15 formulations. When the surfaces of CHX-CP10 and CHX-CP15 are compared before and after SBF treatments, there is mineralization activity in the form of rounded deposits on the surfaces of SBF-treated samples. Elements were analyzed using EDX to confirm remineralization activity on the surface.

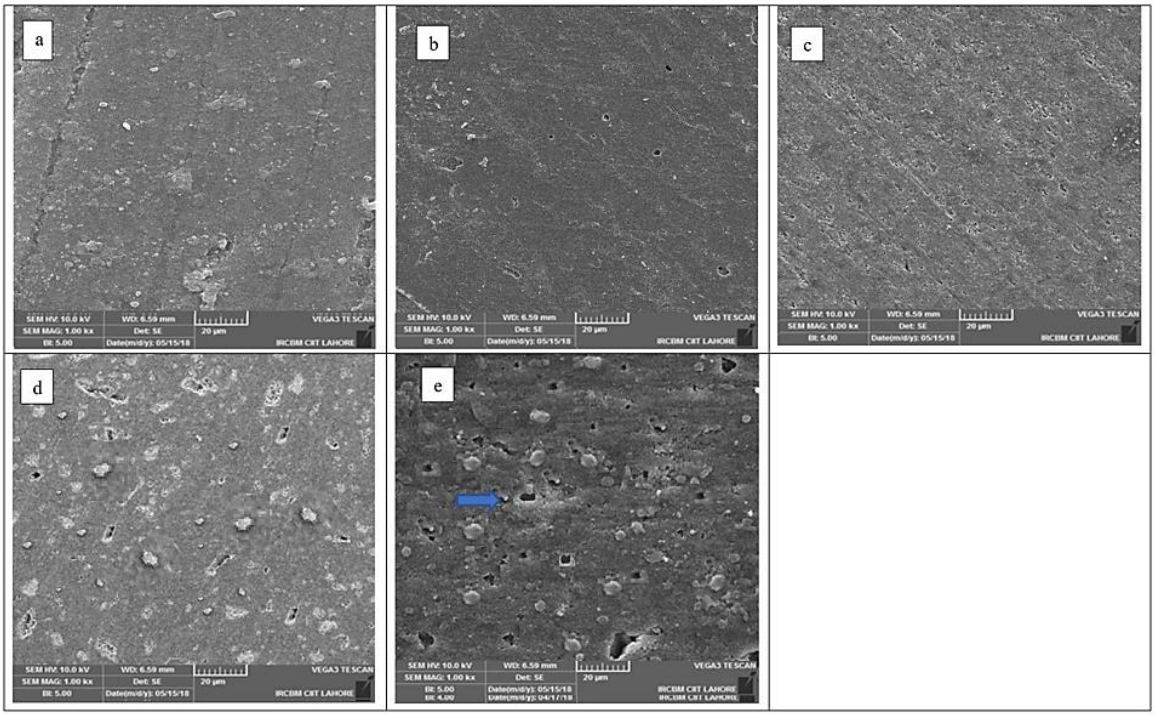

Figure 2. SEM surface analysis of (**a**) Z250, (**b**) BC, (**c**) CHX-CP5, (**d**) CHX-CP10 and (**e**) CHX-CP15 on day 14. The arrow shows mineralization activity in the form of surface deposits. Images at 1000× magnification.

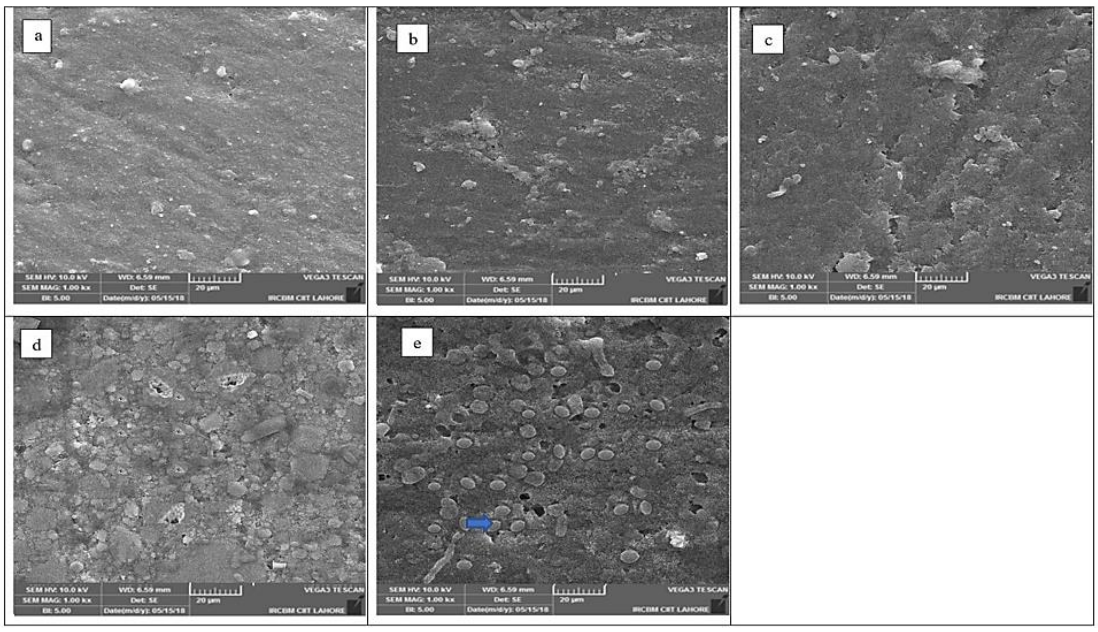

Figure 3. Shows the SEM surface analysis of (**a**) Z250, (**b**) BC, (**c**) CHX-CP5, (**d**) CHX-CP10 and (**e**) CHX-CP15 at day 28. There may be a small deposition of apatite layer as shown by an arrow formation on the surface of CHX-CP10 and CHX-CP15. Images are taken at 1000× magnification.

3.2. EDX Analysis

Figure 4 depicts the elemental surface analysis with EDX for all formulations after 28 days of immersion in SBF. The surface composition of all formulations was silica, oxygen, chloride, calcium, and phosphate. When compared to all experimental formulations, the silica ratio in Z250 was reduced. Furthermore, the calcium and phosphate content

increased as the calcium phosphate filler level increased. The calcium to phosphate ratio of hydroxyapatite is 1.67, but it was 1.9 and 2.0 in CHX-CP10 and CHX-CP15, respectively. EDX demonstrate the presence of calcium and phosphate deposits on the surface of the experimental formulation containing calcium phosphate fillers. The presence of these deposits indicates the presence of some mineralization activity with the highest being observed in group CHX-CP15 as shown in Table 2.

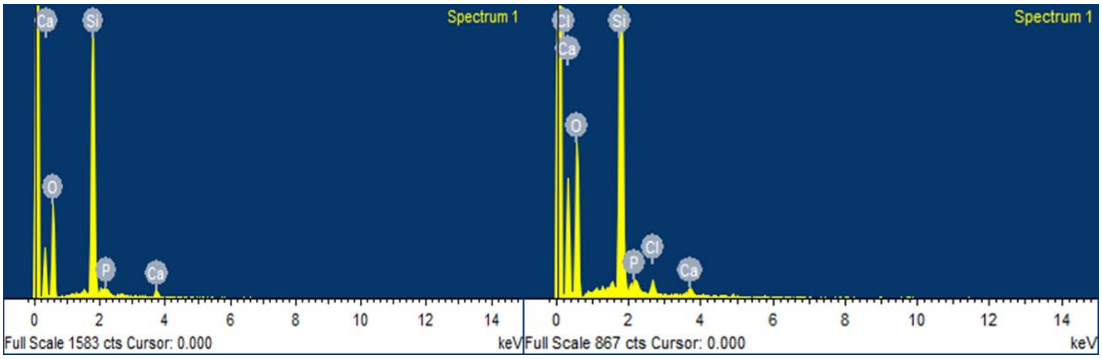

(**a**) (**b**)

Figure 4. EDX spectrum of disc surface of CHX-CP10 and CHX-CP15 after immersion in simulated body fluid for 28 days. (**a**) CHX-CP10; (**b**) CHX-CP15.

Table 2. EDX elemental analysis of the surface of the commercial and experimental formulation after 28 days in SBF.

	Z250		BC		CHX-CP5		CHX-CP10		CHX-CP15	
Element	**Wt%**	**Atomic%**	**Wt%**	**Atomic%**	**Wt%**	**Atomic%**	**Wt%**	**Atomic%**	**Wt%**	**Atomic%**
O [1]	65.60	68.76	58.68	71.35	57.56	70.52	57.54	70.79	56.95	**70.22**
Si [2]	33.95	25.51	42.32	29.31	41.37	28.86	38.90	27.26	38.26	28.24
P [3]	−0.32	−0.23	−1.21	−0.53	0.28	0.46	0.98	0.33	0.52	0.62
Cl [4]	0.45	0.60	0.32	0.10	0.88	0.94	1.74	1.68	1.94	1.70
Ca [5]	0.10	0.15	0.12	0.15	0.40	0.15	1.87	0.54	1.10	0.92
Total	100		100		100		100		100	

[1] Oxygen; [2] Silicon; [3] Phosphate; [4] Chlorine; [5] Calcium.

The strongest peaks are due to calcium and silicon, with weak peaks present for phosphate, chloride, and oxygen.

3.3. Z250 FTIR Spectra Analysis

3.3.1. FTIR Spectra of Z250

FTIR spectra of commercial Z250 of before and after 40 s of light curing shows a strong peak of carbonyl stretch (C=O), observed at 1711–1715 cm^{-1}, commonly associated with BisGMA, BisEMA, UDMA, and TEGDMA. Furthermore, peaks at 1600–1636 cm^{-1} represent the C=C in the aromatic-carbon rings in both BisEMA and BIsGMA. The peak observed at 1510 cm^{-1} was due to the stretching of N-H of urethane dimethacrylate. A peak at 1049 cm^{-1} representing C-O-C and Si-O asymmetric stretching, was due to presence of silicates in the composition. After curing, peak heights of C=O and C=C were reduced. The aromatic and aliphatic group of methacrylate resin decreased at 1606 cm^{-1} and 1636 cm^{-1}, respectively as mentioned in Figure 5. A dominant peak at 1030 cm^{-1} was observed due to the inorganic filler phase.

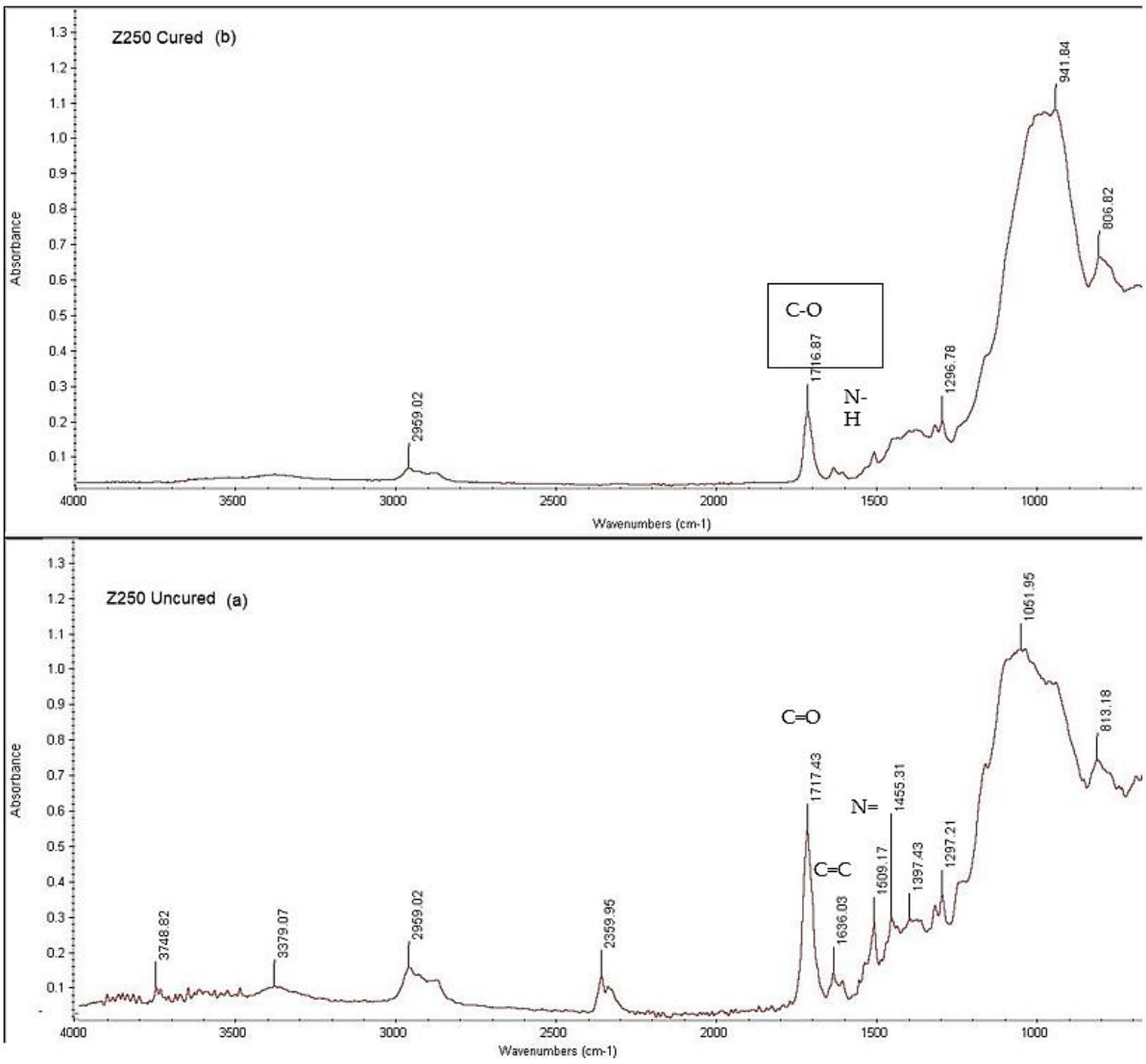

Figure 5. Caption. representative FTIR spectra of Z250 commercial composite before (**a**) and after blue light exposure of 40 s (**b**).

3.3.2. FTIR Spectra of Group BC

All the changes that were observed after curing were characteristics of methacrylate monomer polymerization. Peak 1320 cm^{-1} represents the C-O bond stretching in the methacrylate polymerization reaction. The spectra shows a monomer/polymer peak at 1160 cm^{-1} (C-O-C stretch), 1455 cm^{-1} (C-H bend), 1528 cm^{-1} (N-H deformation), 1636 cm^{-1} (C=C stretch), and 1715 cm^{-1} (C=O stretch) as mentioned in Figure 6. The asymmetric C-H vibration could be observed at 2958 cm^{-1}. C=O stretch observed at peak 1715 cm^{-1} is due to the free monomer in the paste. Symmetric stretching was seen at 1310 cm^{-1}, whereas symmetric carboxylate stretching was observed at 1636 cm^{-1}. After curing, peak heights at 1636 cm^{-1} and 1715 cm^{-1} decreased due to the conversion of double bond into single bond.

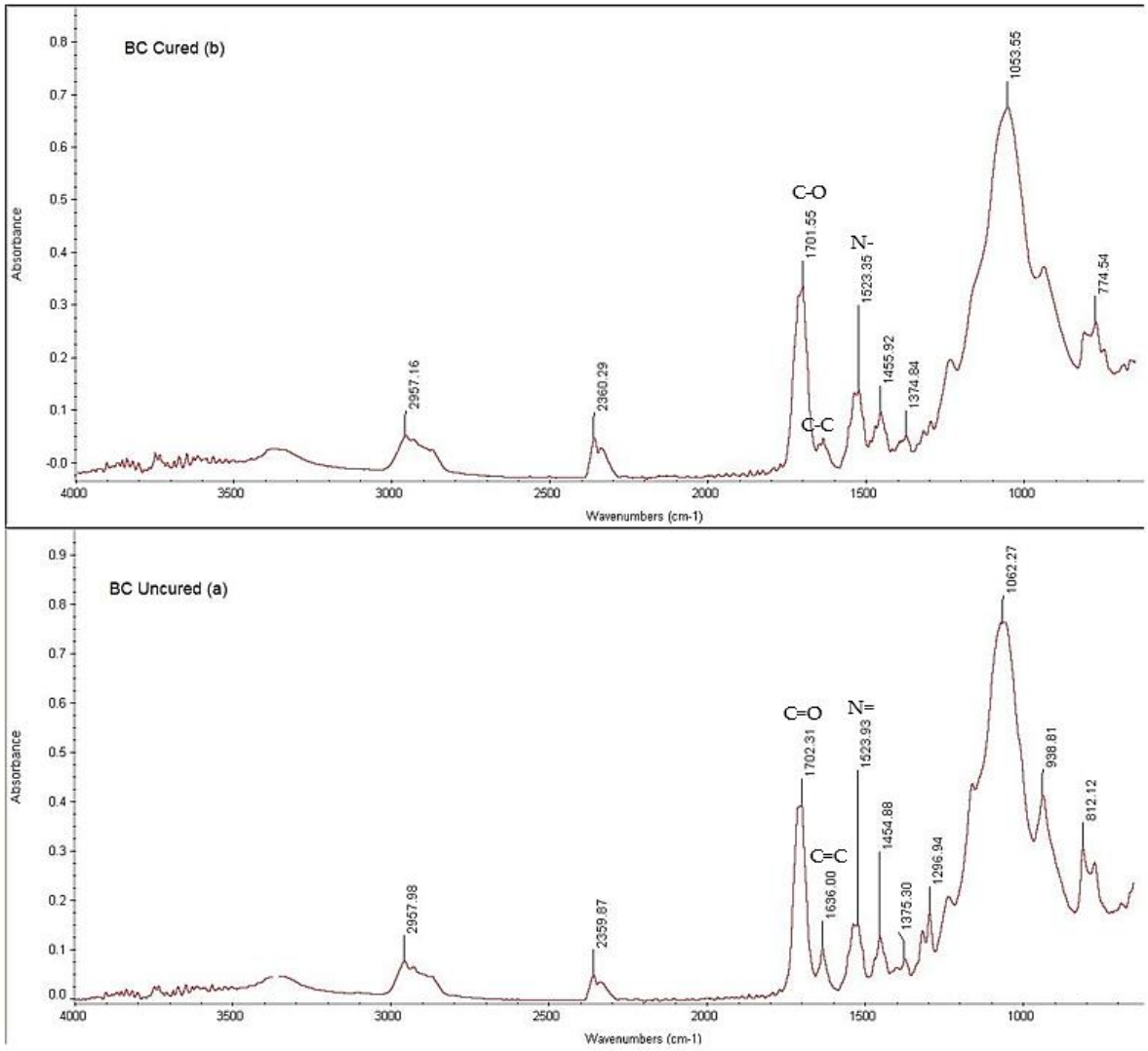

Figure 6. Before (**a**) and after curing for 40 s (**b**) representative FTIR spectra for experimental formulation BC containing only the salinized silica with no added fillers. The 1715 cm^{-1} and 1636 cm^{-1} peaks were decreased upon curing. Group BC contained only silica with no added calcium phosphate filler and chlorhexidine.

3.3.3. FTIR Spectra of Group CHX-CP5

These spectra represent the FTIR spectral analysis of before and after curing for experimental formulations CHX-CP5. All experimental formulations have strong monomer peaks at 1715 cm^{-1} (C=O stretch). Peaks at 1530 cm^{-1} and 1636 cm^{-1} are due to N-H stretch and C=C deformation. Further peaks are observed at 1458 cm^{-1} which is due to the aliphatic C-H vibration. Peaks at 1298 cm^{-1} and 1320 cm^{-1} are associated with C-O stretch, while the peak at 1164 cm^{-1} is due to C-O-C asymmetric stretch. P-O stretch in the spectra at peaks at 1055 cm^{-1} and 940 cm^{-1} are because of mono calcium mono phosphate and tricalcium phosphate, respectively (Figure 7). On the other hand, Silica Glass peak are found at 988 cm^{-1}. CHX levels are too low to detect or its peaks are overlapped by Silica glass peak. After cure, polymerization reaction is initiated and there was a decrease in the intensity of C-O peak (1298 cm^{-1} and 1320 cm^{-1} 1638 cm^{-1}) and C=C peaks (1638 cm^{-1}).

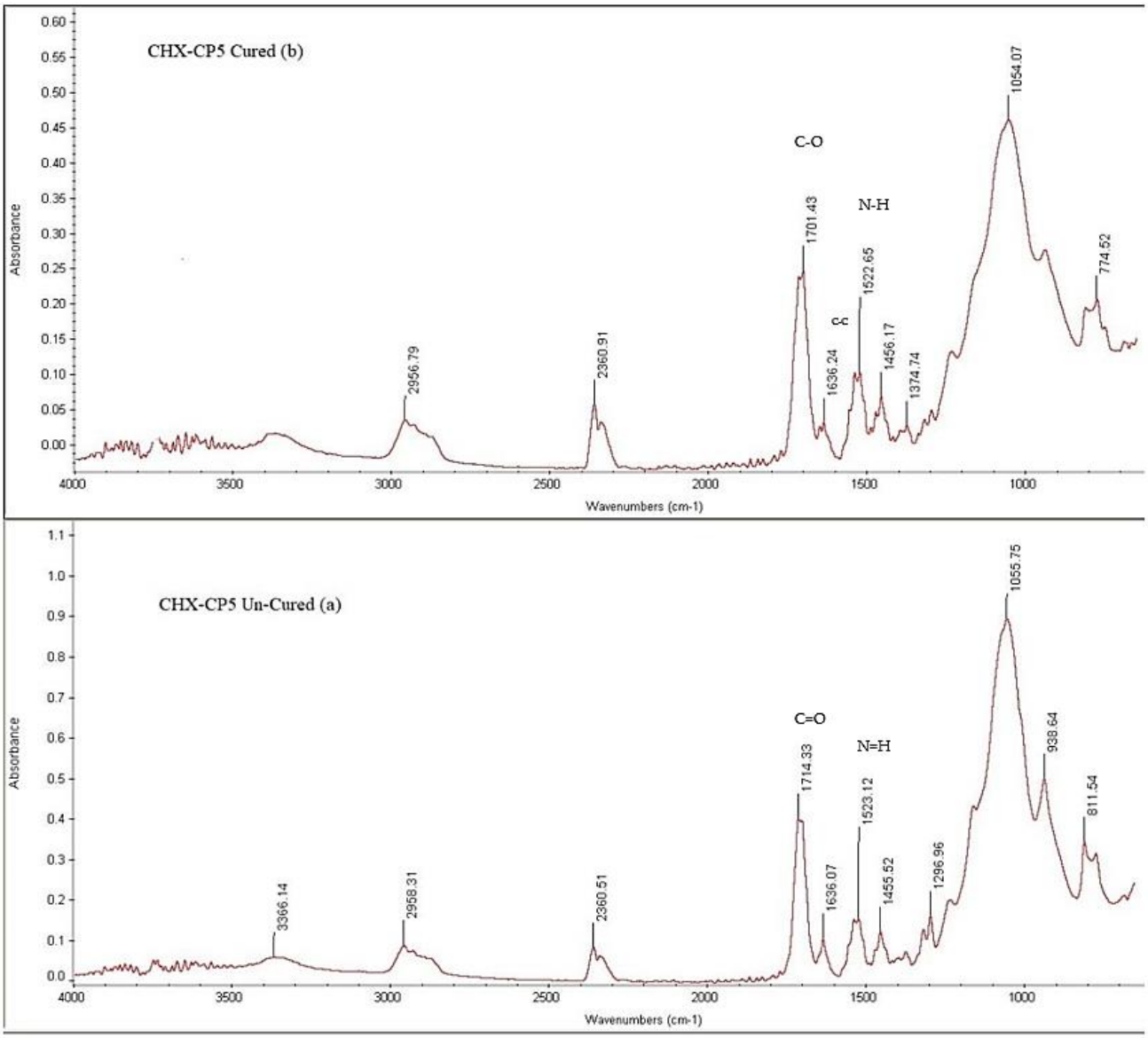

Figure 7. FTIR spectra analysis of the uncured (**a**) and cured (**b**) group CHX-CP5. The peak heights are visible at C=O (1714 cm^{-1}) and P=O (1050 cm^{-1}). Group CHX-CP% filler phase is composed of 5 wt% Chlorhexidine and 5 wt% calcium phosphate fillers.

3.3.4. FTIR Spectra of Group CHX-CP10

FTIR spectra for experimental formulations CHX-CP10 containing 10 wt% CaP and 5 wt% CHX before and after curing for 40 s are shown in Figure 8 All experimental formulations have strong monomer peaks at 1715 cm^{-1} (C=O stretch). Peaks at 1530 cm^{-1} and 1636 cm^{-1} are due to N-H stretch and C=C deformation. Further peaks are observed at 1458 cm^{-1} due to the aliphatic C-H vibration, 1298 and 1320 cm^{-1} associated with a C-O stretch and 1164 cm^{-1} because of a C-O-C asymmetric stretch. P-O stretch in the spectra at peaks at 1055 cm^{-1} and 940 cm^{-1} are because of CPM and TCP, respectively. After the cure, polymerization reaction was initiated and there was a decrease in the intensity of C-O peak (1298 cm^{-1} and 1320 cm^{-1} 1638 cm^{-1}) and C=C peaks (1638 cm^{-1}).

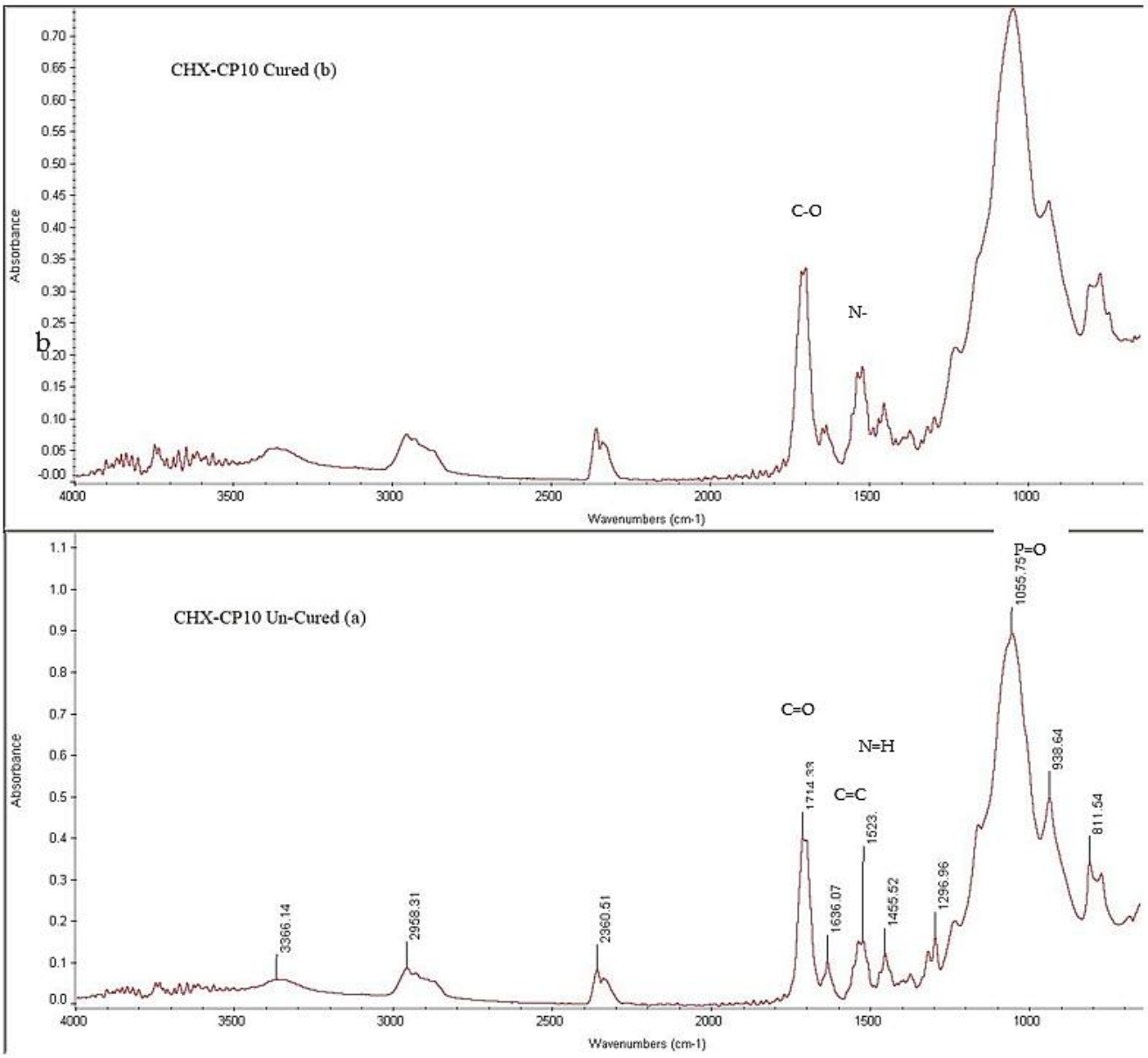

Figure 8. Comparative FTIR spectral image shows the uncured (**a**) and cured (**b**) sample of CHX-CP10. After curing for 40 s, a decrease in the intensity of C-O peak (1298 cm^{-1} and 1320 cm^{-1}) and C=C peaks (1636 cm^{-1}) was observed.

3.3.5. FTIR Spectra of Group CHX-CP15

Figure 9 represents a FTIR spectral analysis of the formulation CHX-CP15 before and after light curing for 40 s. The peak at 1715 cm^{-1} was due to the stretch of C=O group. The spectra also show polymer/monomer peaks at 1636 cm^{-1}, 1529 cm^{-1} (N-H deformation), and 1455 cm^{-1} (C-H bend). TCP and MCPM are represented by the P-O stretch at peak 940 cm^{-1} and 1055 cm^{-1}, respectively. After curing, there was a slight change in peak height recorded at 1320 cm^{-1} and 1636 cm^{-1}.

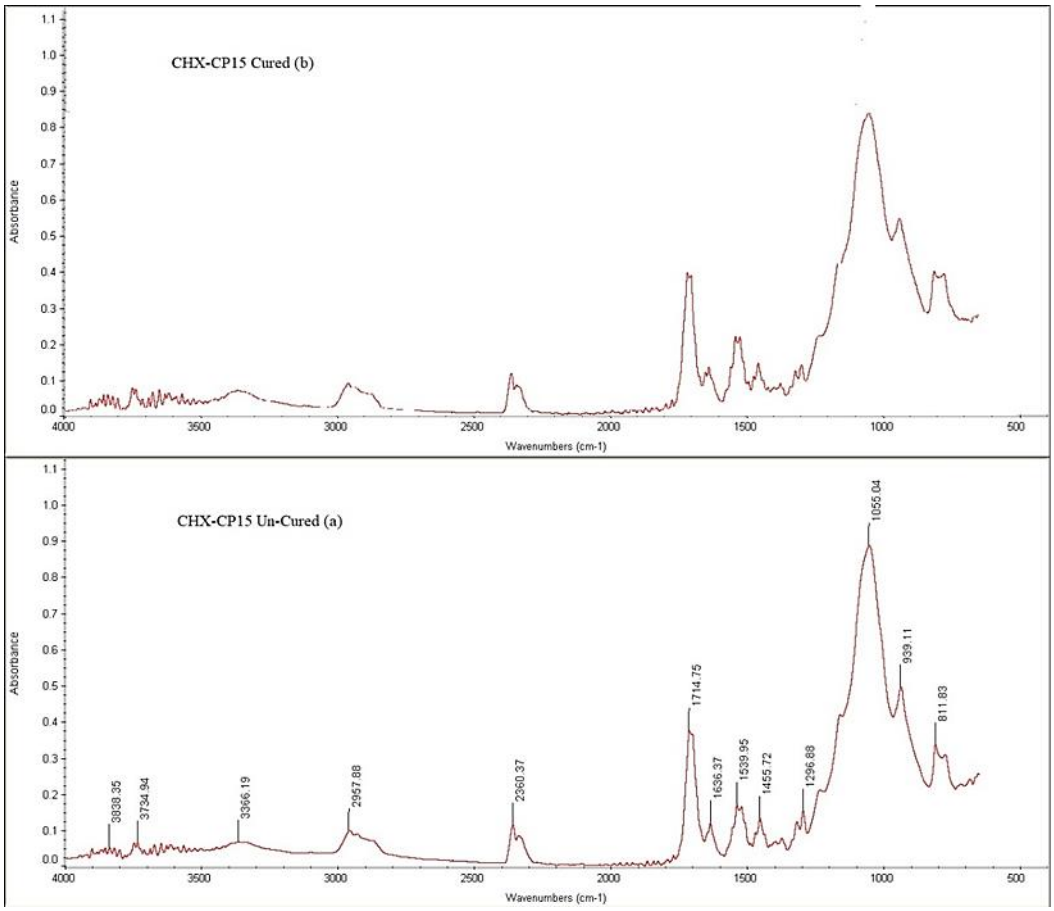

Figure 9. Representative FTIR spectra of CHX-CP15 before and after 40 s of light curing. The various peak such as C=O, Si-O and P-O was represented at 1715 cm^{-1}, 988 cm^{-1}, 1056 cm^{-1}, respectively.

4. Discussion

The current study investigated the in vitro bioactivity of a novel RBDC prepared with reactive calcium phosphate fillers (a mixture of TCP and mono calcium phosphate mono-hydrate) as a remineralizing agent. Aside from calcium phosphate fillers, the newly developed dental composite also contains a mixture of chlorhexidine diacetate and PPG-DMA-based resin. A composite containing chlorhexidine has the potential to inhibit bacterial growth in the vicinity of the restoration [25–27]. Our findings showed mineral deposition with high levels of calcium phosphate fillers. Calcium phosphate fillers have been shown to aid in dentine repair via remineralization [28]. Furthermore, the apatite layer formed by calcium phosphate may inhibit secondary caries propagation, thereby improving the longevity of the restorations [5].

According to research, maximum bioactivity in the form of apatite formation occurs in an SBF (simulated body fluid) environment at 37 °C. Because SBF replicates the conditions of human blood plasma, it has been used as a storage medium for both dental and medical devices [29,30]. SBF acts as a medium, stimulating calcium phosphate's bioactive potential. As a result, bone-like nano-sized deposits with a composition similar to human hard tissues are produced. Although SBF does not contain relevant bioactive compounds such as proteins, it does replicate the inorganic component of human plasma. This is the real difference between biological and induced bone, such as apatite crystals and hard tissue-like inclusions [31]. In our study, samples were immersed in simulated body fluid for 7, 14, and 28 days before being examined using SEM and EDX. Z250 and BC showed no bioactivity or apatite layer formation on day 7. However, SEM images show particle settlement on its surface, as shown in Figure 1a,b.

When calcium phosphate fillers were added to CHX-CP5, CHX-CP10, and CHX-CP15, air bubbles appeared on the surface. Furthermore, the frequency of air bubbles increased as the calcium phosphate filler level increased. This could be due to insufficient wetting of the filler particle, resulting in void formation, or to a difference in particle sizes between MCPM (62 m) and TCP (11 m) [8,32]. The addition of a co-filler with $Ca_3(PO_4)_2$ fillers, such as nano silica-fused silicon carbide whiskers and dimethyl tetrachloroterephthalate nanoparticles, may help to mitigate the weakening effects of $Ca_3(PO_4)_2$ [33].

On day 7, no remineralization layer formed in any of the formulations. Smaller globular deposits were observed on CHX-CP15 and CHX-CP10 on days 14 and 28. These small globular calcium and phosphate deposits on the surface of CHX-CP15 and CHX-CP10 could be formed by SBF or precipitated by a reaction between MCPM and TCP in the presence of water to form brushite, which further changed to probable hydroxyapatite [22]. A previous study demonstrated that adding MCPM and TCP to the surface may enhance the formation of apatite layers [34].

The EDX analysis of the globular deposits confirmed the presence of elements such as silicon, oxygen, calcium, phosphate, and chloride on the surface. The silicate glass/inorganic filler particles are represented by the silicone. While the calcium, phosphate, and chloride that settles on the surface can emerge from either the SBF solution or the composite surface (MCPM/ TCP). Further to that, the calcium and phosphate levels on the surface have increased as the calcium phosphate fillers have increased. The higher the calcium and phosphate concentrations, hence more bone-like apatite phase precipitates. Ca/P ratios in HA are typically around 1.67 (1.5–1.7) [35].

However, the current research found a ratio of 1.9–2.0. The higher the Ca/P ratio, the more likely it is to be carbonate apatite, in which phosphate $(PO_4)^{3-}$ substitutes for carbonate $(CO_3)^{2-}$, which typically occurs during biological processes [36].

5. Limitations of the Study

The varying concentrations of TCP, MCPM, and chlorhexidine, which could have been adjusted to reduce porosities, were the study's limiting factors. Furthermore, the properties were assessed in simulated body fluid and artificial saliva for a limited time. Multiple forces are applied dynamically in the oral cavity, so mechanical properties should be assessed using flexural and fatigue strength tests to measure stress in both flexion and tension at various time points. The recommendations for future work include evaluating the degree of conversion, mechanical properties at 1-, 3-, and 6-month intervals, as well as in vivo bioactivity and cytotoxicity. It is anticipated that any further investigation into these aspects will improve the study's validity.

6. Conclusions

Calcium phosphate fillers loading enhances the remineralizing properties of novel dental resin composites. Maximum calcium phosphate/apatite deposition was observed after immersion in SBF in the group containing 15% monocalcium phosphate monohydrate and tri calcium phosphate (CHX-CP 15) with the highest level of calcium phosphate filler, i.e., CHX-CP15 > CHX-CP10. In contrast, no apatite layer deposition was observed in the commercial (Z250), basic composite (BC), and 5% monocalcium phosphate monohydrate and dicalcium phosphate dihydrate groups (CHX-CP5). The emergence of an apatite-like layer on the surface of calcium phosphate-loaded novel dental composites may indicate the novel composite system's prospective remineralizing ability.

Author Contributions: Conceptualization, Z.S. and M.A.K.; methodology, Z.S. and N.M.; software, Z.S. and N.M.; validation, N.I. and M.S.Z.; formal analysis, N.I.; investigation, Z.S. and N.M.; resources, N.I.; data curation, Z.S., M.A.K. and N.I. writing—original draft preparation, Z.S. and N.M.; writing—review and editing, M.S.Z. and M.A.F.; supervision and project administration, M.A.K. All authors have read and agreed to the published version of the manuscript.

Funding: This research received no external funding.

Institutional Review Board Statement: The study was conducted in accordance with the Declaration of Helsinki, and approved by the Institutional Review Board (or Ethics Committee) of PGMI. It was an in-vitro study which do not involve human/animal subjects. Therefore an informal letter was issued by the institute.which was attached during submission.

Informed Consent Statement: Not applicable.

Data Availability Statement: Data is confidential as per the institute's policy will be provided on request.

Acknowledgments: The authors are obliged and thankful to Nawshad Muhammad and Faiza IRCBM, CUI, Lahore Campus, Islamabad Pakistan for the assistance and support. All the individuals have consented to the acknowledgments.

Conflicts of Interest: The authors declare no conflict of interest.

References

1. Alcaraz, M.G.R.; Veitz-Keenan, A.; Sahrmann, P.; Schmidlin, P.R.; Davis, D.; Iheozor-Ejiofor, Z. Direct composite resin fillings versus amalgam fillings for permanent or adult posterior teeth. *Cochrane Database Syst. Rev.* **2014**, *31*. [CrossRef]
2. Munir, N.; Inayat, N.; Qaiser, A.; Khan, S.A.; Rana, M.H. Evaluation of the Integrity of Amalgam-Composite Interface with Two Resin Based Intermediate Materials. *J. Bahria Univ. Med. Dent. Coll.* **2017**, *7*, 119–124.
3. Khan, A.A.; Zafar, M.S.; Ali A Ghubayri, A.; AlMufareh, N.A.; Binobaid, A.; Eskandrani, R.M.; Al-Kheraif, A.A. Polymerisation of restorative dental composites: Influence on physical, mechanical and chemical properties at various setting depths. *Mater. Technol.* **2022**, *37*, 2056–2062. [CrossRef]
4. Cramer, N.B.; Stansbury, J.W.; Bowman, C.N. Recent advances and developments in composite dental restorative materials. *J. Dent. Res.* **2011**, *90*, 402–416. [CrossRef]
5. Alfawaz, Y.F.; Almutairi, B.; Kattan, H.F.; Zafar, M.S.; Farooq, I.; Naseem, M.; Vohra, F.; Abduljabbar, T. Dentin bond integrity of hydroxyapatite containing resin adhesive enhanced with graphene oxide nano-particles—An SEM, EDX, micro-raman, and microtensile bond strength study. *Polymers* **2020**, *12*, 2978. [CrossRef]
6. Ali, S.; Sangi, L.; Kumar, N.; Kumar, B.; Khurshid, Z.; Zafar, M.S. Evaluating antibacterial and surface mechanical properties of chitosan modified dental resin composites. *Technol. Health Care* **2020**, *28*, 165–173. [CrossRef]
7. Braun, H.; Zonta, J.H.; Soares de Souza Lima, J.; Fialho dos Reis, E. Produção De Mudas De Café 'Conilon' Propagadas Vegetativamente Em Diferentes Níveis De Sombreamento. *Idesia* **2007**, *25*, 184–194. [CrossRef]
8. Aljabo, A.; Abou Neel, E.A.; Knowles, J.C.; Young, A.M. Development of dental composites with reactive fillers that promote precipitation of antibacterial-hydroxyapatite layers. *Mater. Sci. Eng. C* **2016**, *60*, 285–292. [CrossRef]
9. Walters, N.J.; Xia, W.; Salih, V.; Ashley, P.F.; Young, A.M. Poly(propylene glycol) and urethane dimethacrylates improve conversion of dental composites and reveal complexity of cytocompatibility testing. *Dent. Mater.* **2016**, *32*, 264–277. [CrossRef]
10. Delgado, A.H.S.; Owji, N.; Ashley, P.; Young, A.M. Varying 10-methacryloyloxydecyl dihydrogen phosphate (10-MDP) level improves polymerisation kinetics and flexural strength in self-adhesive, remineralising composites. *Dent. Mater.* **2021**, *37*, 1366–1376. [CrossRef]
11. Agrawal, S.; Srivastava, R. Osteoinductive and osteoconductive biomaterials. In *Racing for the Surface: Antimicrobial and Interface Tissue Engineering*; Springer: Berlin, Germany, 2020; pp. 355–395.
12. Alshami, A.A. Development of a Novel Antibacterial and Remineralising Dental Composite for Paediatric Dentistry. Ph.D. Thesis, University College London, London, UK, 2015; 310p.
13. Bohner, M. Calcium orthophosphates in medicine: From ceramics to calcium phosphate cements. *Injury* **2000**, *31* (Suppl. S4), 37–47. [CrossRef] [PubMed]
14. Lodoso-Torrecilla, I.; van den Beucken, J.J.J.P.; Jansen, J.A. Calcium phosphate cements: Optimization toward biodegradability. *Acta Biomater.* **2021**, *119*, 1–12. [CrossRef] [PubMed]
15. Reif, S.C. Dedicated To. *Vetus Testam.* **1972**, *22*, 495–501. [CrossRef]
16. Al-Sanabani, J.S.; Madfa, A.A.; Al-Sanabani, F.A. Application of calcium phosphate materials in dentistry. *Int. J. Biomater.* **2013**, *2013*. [CrossRef]
17. Suzuki, O.; Shiwaku, Y.; Hamai, R. Octacalcium phosphate bone substitute materials: Comparison between properties of biomaterials and other calcium phosphate materials. *Dent. Mater. J.* **2020**, *39*, 187–199. [CrossRef]
18. Momma, K.; Izumi, F. VESTA 3 for three-dimensional visualization of crystal, volumetric and morphology data. *J. Appl. Crystallogr.* **2011**, *44*, 1272–1276. [CrossRef]
19. Khan, A.S.; Syed, M.R. A review of bioceramics-based dental restorative materials. *Dent. Mater. J.* **2019**, *38*, 163–176. [CrossRef]
20. Almulhim, K.S.; Syed, M.R.; Alqahtani, N.; Alamoudi, M.; Khan, M.; Ahmed, S.Z.; Khan, A.S. Bioactive Inorganic Materials for Dental Applications: A Narrative Review. *Materials* **2022**, *15*, 6864. [CrossRef]
21. Cheng, L.; Weir, M.D.; Xu, H.H.K.; Kraigsley, A.M.; Lin, N.J.; Lin-Gibson, S.; Zhou, X. Antibacterial and physical properties of calcium-phosphate and calcium-fluoride nanocomposites with chlorhexidine. *Dent. Mater.* **2012**, *28*, 573–583. [CrossRef]

22. Yoruç, A.B.H.; Aydınoğlu, A. The precursors effects on biomimetic hydroxyapatite ceramic powders. *Mater. Sci. Eng. C* **2017**, *75*, 934–946. [CrossRef]
23. Kokubo, T.; Takadama, H. How useful is SBF in predicting in vivo bone bioactivity? *Biomaterials* **2006**, *27*, 2907–2915. [CrossRef] [PubMed]
24. Yilmaz, B.; Pazarceviren, A.E.; Tezcaner, A.; Evis, Z. Historical development of simulated body fluids used in biomedical applications: A review. *Microchem. J.* **2020**, *155*, 104713. [CrossRef]
25. Beyth, N.; Houri-Haddad, Y.; Domb, A.; Khan, W.; Hazan, R. Alternative antimicrobial approach: Nano-antimicrobial materials. *Evid. Based Complement. Altern. Med.* **2015**, *2015*. [CrossRef] [PubMed]
26. Mehdawi, I.M.; Kitagawa, R.; Kitagawa, H.; Yamaguchi, S.; Hirose, N.; Kohno, T.; Imazato, S. Incorporation of chlorhexidine in self-adhesive resin cements. *Dent. Mater. J.* **2022**, *41*, 675–681. [CrossRef]
27. Amin, F.; Fareed, M.A.; Zafar, M.S.; Khurshid, Z.; Palma, P.J.; Kumar, N. Degradation and Stabilization of Resin-Dentine Interfaces in Polymeric Dental Adhesives: An Updated Review. *Coatings* **2022**, *12*, 1094. [CrossRef]
28. Par, M.; Gubler, A.; Attin, T.; Tarle, Z.; Tarle, A.; Prskalo, K.; Tauböck, T. Effect of adhesive coating on calcium, phosphate, and fluoride release from experimental and commercial remineralizing dental restorative materials. *Sci. Rep.* **2022**, *12*, 10272. [CrossRef]
29. Baino, F.; Yamaguchi, S. The use of simulated body fluid (SBF) for assessing materials bioactivity in the context of tissue engineering: Review and challenges. *Biomimetics* **2020**, *5*, 57. [CrossRef]
30. Dridi, A.; Riahi, K.Z.; Somrani, S. Mechanism of apatite formation on a poorly crystallized calcium phosphate in a simulated body fluid (SBF) at 37 °C. *J. Phys. Chem. Solids* **2021**, *156*, 110122. [CrossRef]
31. Díaz-Cuenca, A.; Rabadjieva, D.; Sezanova, K.; Gergulova, R.; Ilieva, R.; Tepavitcharova, S. Biocompatible calcium phosphate-based ceramics and composites. *Mater. Today Proc.* **2022**, *61*, 1217–1225. [CrossRef]
32. Engstrand, J.; Persson, C.; Engqvist, H. The effect of composition on mechanical properties of brushite cements. *J. Mech. Behav. Biomed. Mater.* **2014**, *29*, 81–90. [CrossRef]
33. Elfakhri, F.; Alkahtani, R.; Li, C.; Khaliq, J. Influence of filler characteristics on the performance of dental composites: A comprehensive review. *Ceram. Int.* **2022**, *48*, 27280–27294. [CrossRef]
34. Panpisut, P.; Suppapatpong, T.; Rattanapan, A.; Wongwarawut, P. Monomer conversion, biaxial flexural strength, apatite forming ability of experimental dual-cured and self-adhesive dental composites containing calcium phosphate and nisin. *Dent. Mater. J.* **2021**, *40*, 399–406. [CrossRef]
35. Senra, M.R.; de Lima, R.B.; Souza, D.D.H.S.; Marques, M.D.F.V.; Monteiro, S.N. Thermal characterization of hydroxyapatite or carbonated hydroxyapatite hybrid composites with distinguished collagens for bone graft. *J. Mater. Res. Technol.* **2020**, *9*, 7190–7200. [CrossRef]
36. Yang, L.; Perez-Amodio, S.; Barrère-de Groot, F.Y.F.; Everts, V.; van Blitterswijk, C.A.; Habibovic, P. The effects of inorganic additives to calcium phosphate on in vitro behavior of osteoblasts and osteoclasts. *Biomaterials* **2010**, *31*, 2976–2989. [CrossRef] [PubMed]